

Bruno de Almeida Lopes<sup>1</sup>, Claus Meyer<sup>2</sup>, Luana Batista<sup>1</sup>, Thayana da Conceição Barbosa<sup>1</sup>, Caroline Pires Poubel<sup>1</sup>, Nicolas Duployez<sup>3</sup>, Udo zur Stadt<sup>4</sup>, Martin Hortsman<sup>4,5</sup>, Chiara Palmi<sup>6</sup>, Giovanni Cazzaniga<sup>6</sup>, Nicola C. Venn<sup>7</sup>, Susan Heatley<sup>8</sup>, Deborah L. White<sup>8,9</sup>, Rosemary Sutton<sup>7</sup>, Barbara Costa Peixoto<sup>10</sup>, Martin Bonamino<sup>10</sup>, Maria S. Pombo-de-Oliveira<sup>1</sup>, Rolf Marschalek<sup>2</sup>, Mariana Emerenciano<sup>1</sup>

<sup>1</sup>Pediatric Hematology-Oncology Program, Research Center, Instituto Nacional de Câncer, Rio de Janeiro, RJ, Brazil; <sup>2</sup>Diagnostic Center of Acute Leukemia/ Institute of Pharmaceutical Biology/ZAFES, Goethe-University of Frankfurt, Biocenter, Max-von-Laue-Str. 9, D-60438 Frankfurt/Main, Germany; <sup>3</sup>Laboratory of Hematology and Tumor Bank, INSERM UMR-S 1172, Cancer Research Institute of Lille, CHRU of Lille, University Lille Nord de France, Lille 59037, France; <sup>4</sup>Center for Diagnostic, University Medical Center Hamburg Eppendorf, Martinistr. 52, Hamburg, Germany; <sup>5</sup>Research Institute Children's Cancer Center, Hamburg, Germany; <sup>6</sup>Department of Pediatric Hematology and Oncology, University Medical Center Hamburg-Eppendorf, Hamburg, Germany; <sup>7</sup>Centro Ricerca Tettamanti, Clinica Pediatrica, Dipartimento di Medicina e Chirurgia, Università degli Studi di Milano-Bicocca, Fondazione MBBM, Monza, Italy; <sup>8</sup>Children's Cancer Institute, Lowy Cancer Research Centre UNSW, Sydney, New South Wales, Australia; <sup>9</sup>South Australian Health and Medical Research Institute (SAHMRI), Adelaide, South Australia, Australia; <sup>10</sup>Discipline of Medicine, University of Adelaide, Adelaide, South Australia, Australia; <sup>11</sup>Program of Molecular Carcinogenesis, Research Center, Instituto Nacional de Câncer, Rio de Janeiro, RJ, Brazil

## INTRODUCTION

*IKZF1* deletion ( $\Delta IKZF1$ ) is an important predictor of relapse in childhood B-cell precursor acute lymphoblastic leukemia (BCP-ALL). Therefore, PCR systems to generate a rapid identification of  $\Delta IKZF1$  are of clinical importance. We previously mapped the breakpoints of intragenic deletions and developed a multiplex PCR (MP-PCR) assay to detect  $\Delta IKZF1$  ( $\Delta 2-3$ ,  $\Delta 2-7$ ,  $\Delta 2-8$ ,  $\Delta 4-7$ ,  $\Delta 4-8$ ). Because this assay was not able to detect other types of  $\Delta IKZF1$ , we first investigated the genetic scenario of *IKZF1*  $\Delta 1-8$ , and revealed that monosomy 7 and large interstitial deletions on chromosome 7 are the main causes of *IKZF1*  $\Delta 1-8$ . Detailed genomic breakpoint analysis showed that 13% of patients with *IKZF1*  $\Delta 1-8$  had large interstitial deletions starting within *Cordon-Bleu* gene (*COBL*), which is ~611 Kb downstream of *IKZF1*. *COBL* rearrangements (*COBL-r*) lead to both *IKZF1* complete deletions and tail-to-tail fusions between *IKZF1-COBL*. In order to improve the coverage of the MP-PCR assay for detection of  $\Delta IKZF1$ , we aimed at investigating the characteristics of other intragenic deletions. Also, we settled an international collaboration in order to better characterize *COBL-r* in leukemia, and to explore the oncogenic role of alterations between *IKZF1* and *COBL*.

## METHODS

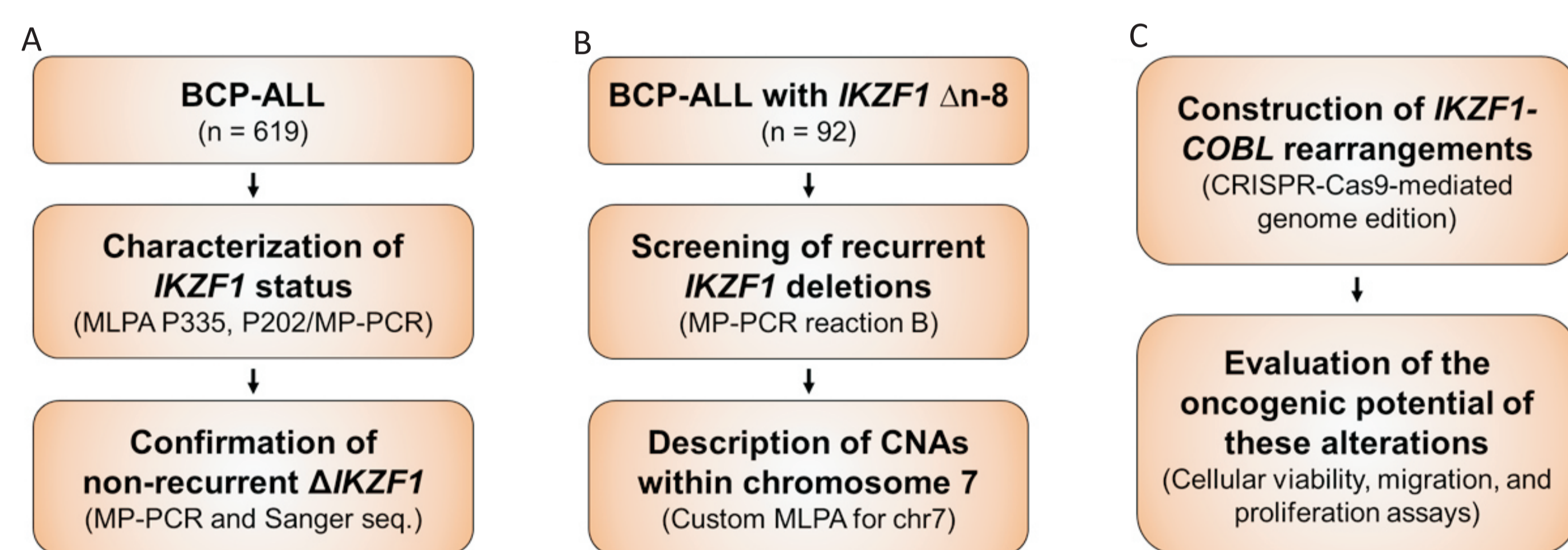


**Figure 1.** This study is divided into three parts. (A) We investigated patients with BCP-ALL and  $\Delta IKZF1$ , which was evaluated by multiplex ligation-dependent probe amplification (MLPA) P335 and confirmed using MLPA P202. PCR amplification of sequences flanking  $\Delta IKZF1$  will be used for mapping breakpoint hotspots. (B) We studied BCP-ALL with *IKZF1*  $\Delta n-8$ . Patients without recurrent deletions ( $\Delta 2-8$ ,  $\Delta 4-8$ ) were evaluated by a customized MLPA for the detection of copy number alterations within chromosome 7. (C) We performed the CRISPR-Cas9-mediated genome edition model for the construction of *IKZF1-COBL* rearrangements, and will evaluate oncogenic potential of these alterations.

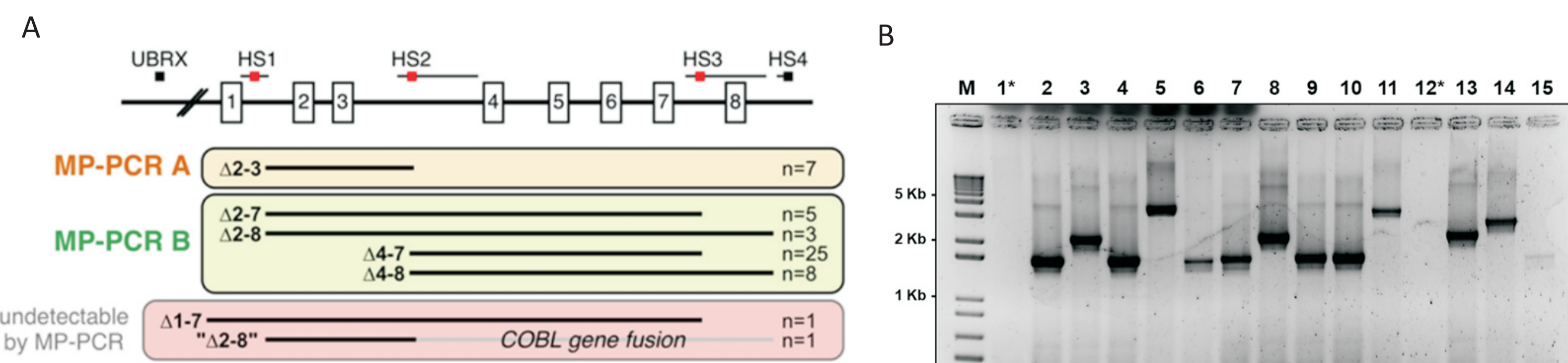


**Figure 2.** We screened recurrent *IKZF1* deletions ( $\Delta 2-8$ ,  $\Delta 4-8$ ) using MP-PCR, reaction B. (A) Four different recombination hotspots (HS1-4) and a single upstream breakpoint (UBRX) are described within *IKZF1*. MP-PCR reactions A and B can identify the most frequent *IKZF1* deletions, respectively. (B) We used the MP-PCR reaction B in order to identify recurrent  $\Delta n-8$  *IKZF1*. Certain samples (\*) did not present recurrent deletions, and were further analyzed by custom MLPA. M, 1 Kb ladder; 1-15, samples with either  $\Delta 2-8$  or  $\Delta 4-8$  as characterized by SALSA MLPA P335/P202.

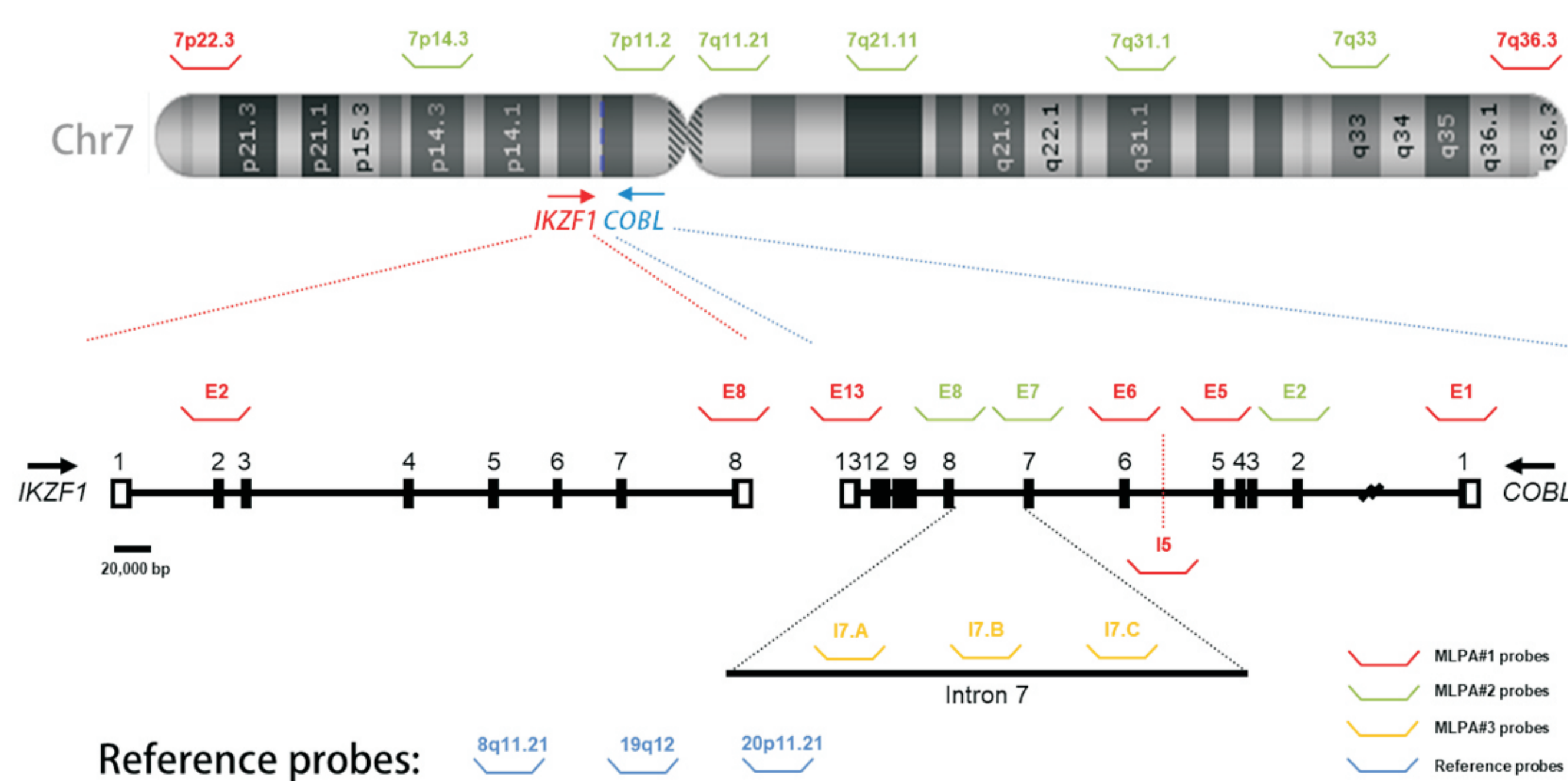


**Figure 3.** Custom MLPA strategy for analysis of copy-number alterations (CNAs) within chromosome 7. Three MLPA assays were used for analyses, and they were composed by MLPA#1 (red), MLPA#2 (green), MLPA#3 (orange) probes mixed with reference probes (blue) located on chromosomes with rare aberrations in BCP-ALL. E, exon; I, intron.

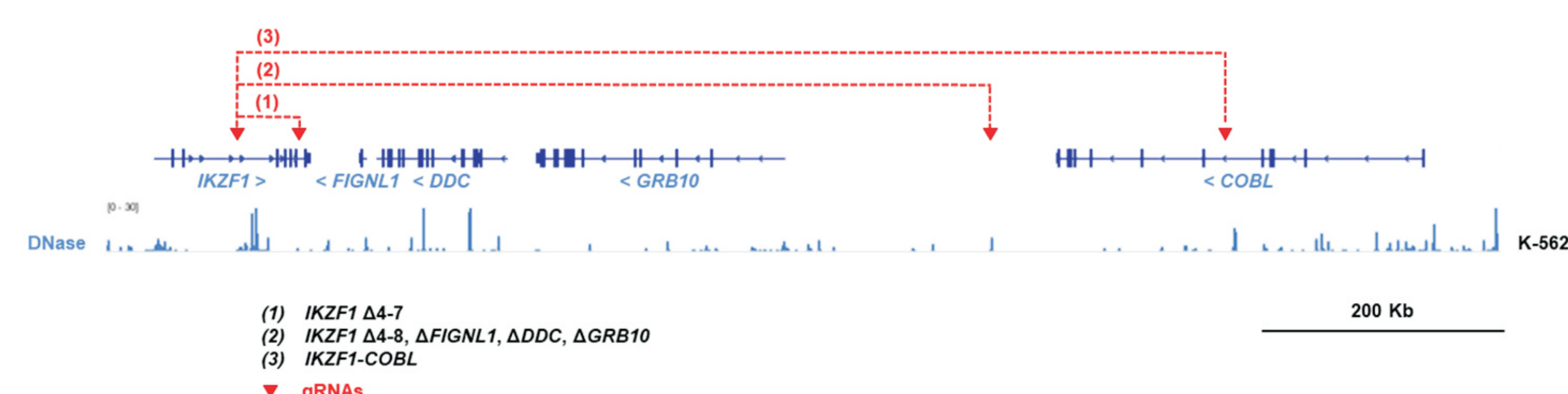


**Figure 4.** For the experimental assays, we performed the CRISPR-Cas9-mediated genome edition model for the construction of rearrangements that mimic (1) the most frequent intragenic deletion of *IKZF1* (*IKZF1*  $\Delta 4-7$ ), (2) the loss of *FIGLN1* and *GRB10* (located between *IKZF1* and *COBL*), and (3) the *IKZF1-COBL* tail-to-tail fusion. The guide RNAs (gRNAs) were designed preferentially within DNase highly sensitive sites of K-562 cell line (ENCODE database).

## RESULTS

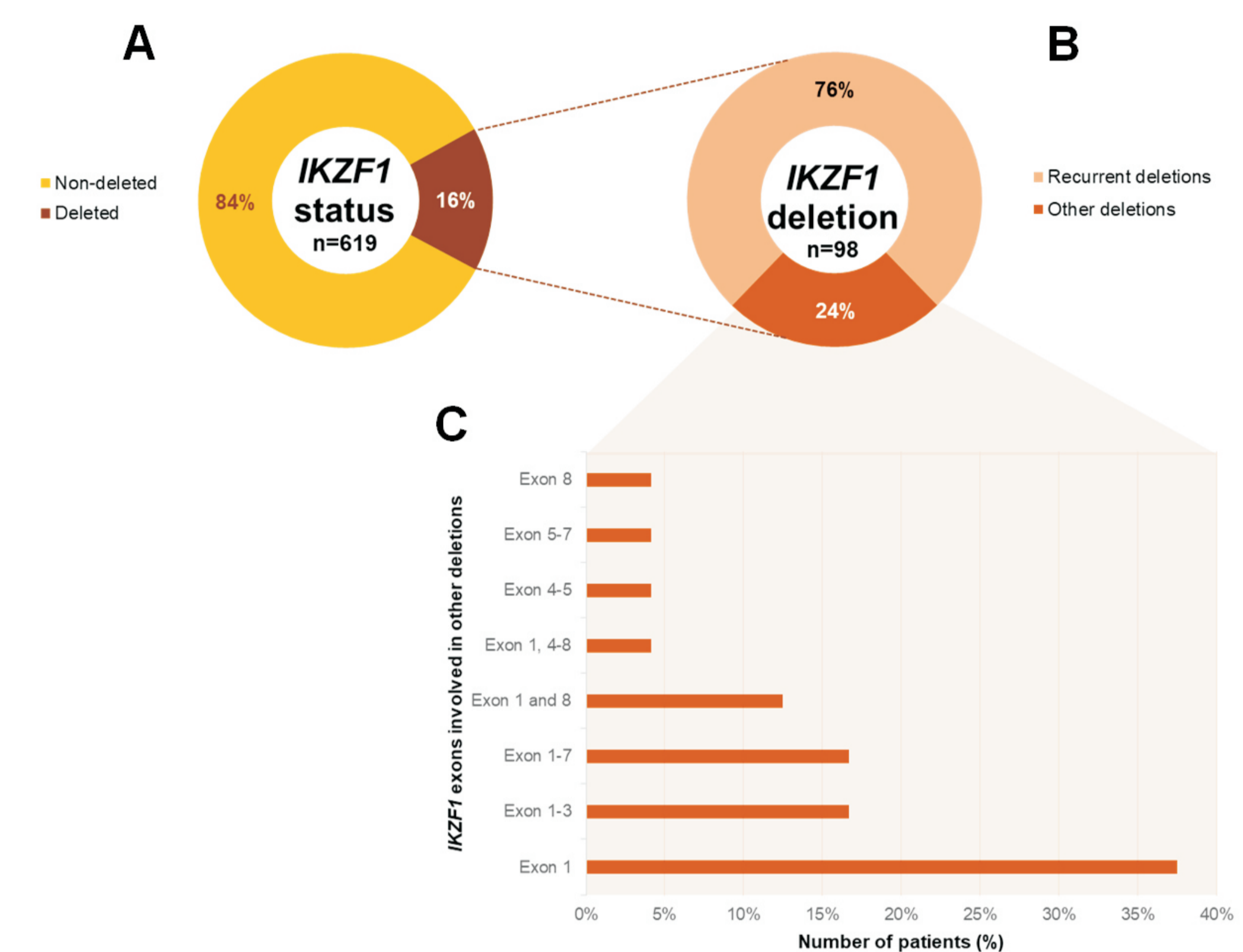


**Figure 5.** Overview of *IKZF1* deletions in childhood BCP-ALL. (A) *IKZF1* deletions were found in 16% of patients with BCP-ALL. (B) Although most of the patients with *IKZF1* deletions displayed recurrent deletions ( $\Delta 1-8$ ,  $\Delta 2-3$ ,  $\Delta 2-7$ ,  $\Delta 2-8$ ,  $\Delta 4-7$ ,  $\Delta 4-8$ ), 24% of them presented other types of deletions, which were characterized by (C) miscellaneous deletions:  $\Delta 1-3$  (17%),  $\Delta 1-7$  (17%), 4-5 (4%),  $\Delta 5-7$  (4%), and one-exon deletions (58%). Most of the one-exon deletions ranged from *IKZF1* promoter until exon 1.

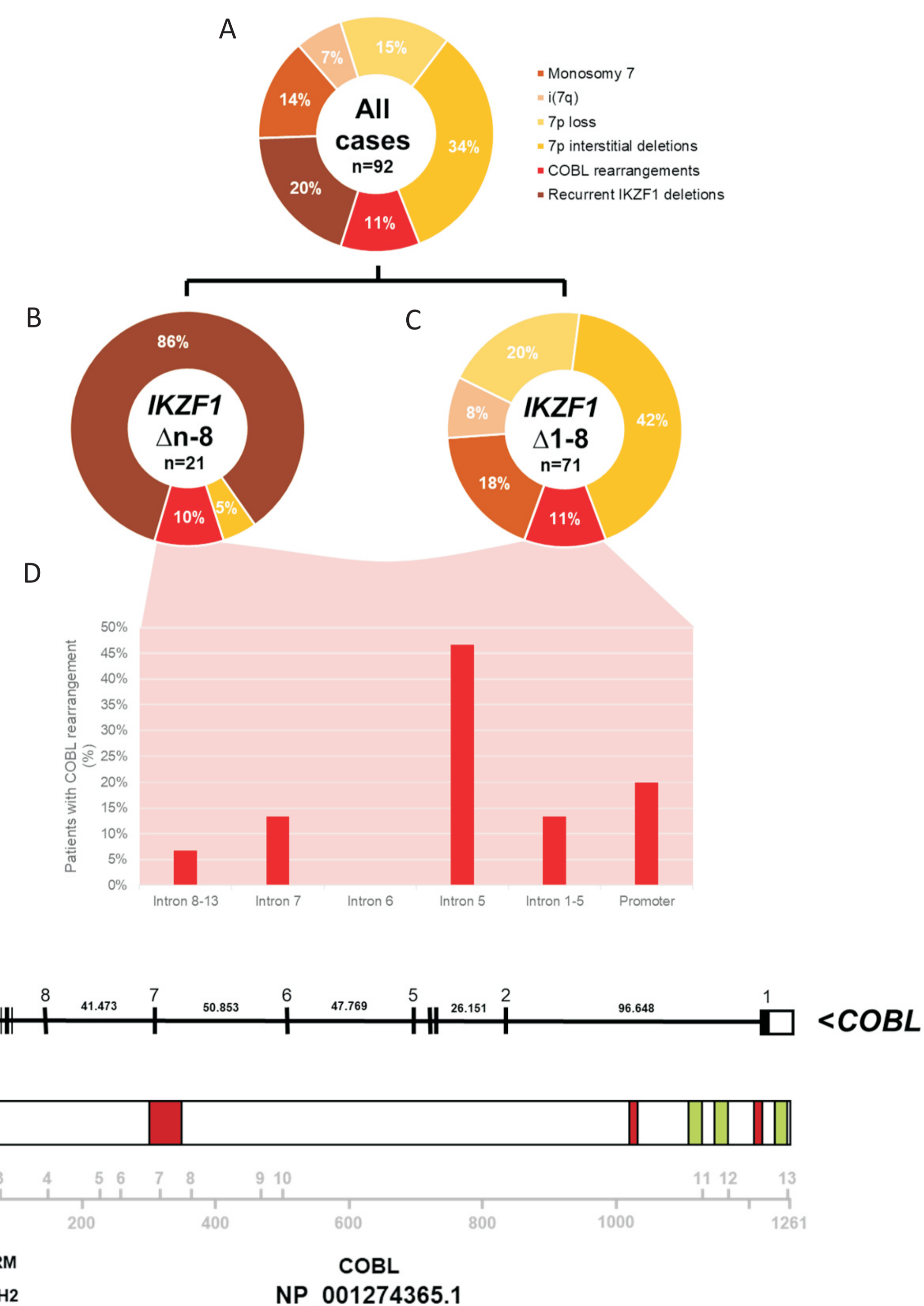


**Figure 6.** Chromosome 7 alterations in patients with *IKZF1*  $\Delta n-8$  are represented for (A) all cases with BCP-ALL, (B) *IKZF1*  $\Delta n-8$  ( $\Delta 2-8$ ,  $\Delta 3-8$ ,  $\Delta 4-8$ ,  $\Delta 6-8$ ), and (C) complete *IKZF1* deletions ( $\Delta 1-8$ ). (D) In total, 15 patients had *IKZF1* deletions with *COBL-r*, and their breakpoints located close to *COBL* promoter (20%) or within its gene-body (80%), mainly on *COBL* intron 5 (47%) and intron 7 (13%). (E) Structure of *COBL*, which is composed of 13 exons and is located on the minus DNA strand. (F) *COBL* protein and its proline-rich (PRM, red), and WASP homology domains (green), which are important for its role on acting nucleation. Protein domain information retrieved from UniProt: *COBL* (O75128).

## CONCLUSION

*IKZF1* deletions are characterized by a diverse spectrum of alterations. Although 26% of intragenic deletions are not detected by MP-PCR methods, we show that this group deserves special attention in order to define its importance for diagnosis and risk stratification. Besides, we have shown that deletions involving exon 8 differ according to the type of *IKZF1* deletion; while intragenic deletions ( $\Delta n-8$ ) present a breakpoint hotspot ~11.6 Kb downstream *IKZF1*, complete deletions ( $\Delta 1-8$ ) are defined by monosomy 7, 7p loss, and interstitial deletions involving *COBL*.